U.S. DEPARTMENT OF COMMERCE
NATIONAL OCEANIC AND ATMOSPHERIC ADMINISTRATION
NATIONAL WEATHER SERVICE
NATIONAL METEOROLOGICAL CENTER

OFFICE NOTE 70

An Oscillation in the NMC Primitive Equation Model

Prior to August 1971

John A. Brown, Jr.
Development Division

JANUARY 1972

ABSTRACT

Primarily as a matter of record, this note documents an investigation which was directed at understanding a problem which existed in the operational primitive equation model of the National Meteorological Center (NMC) prior to August 23, 1971. A diagnostic study of the performance of the six-layer model revealed a persistent type of error in the forecasts. It manifested itself as an initial increase in kinetic energy with an ensuing ten-hour period oscillation. Part of the generating mechanism of this feature was found to reside in the method of data initialization.

1. Introduction

In analyzing the performance of the operational (prior to August 23, 1971) primitive equation forecasting model of the National Meteorological Center (Shuman and Hovermale, 1968), a persistent type of error was discovered in the daily forecasts. During the first 8 to 10 hours of the forecast, the average kinetic energy increased approximately 9 percent. An oscillation with a period of about 10 hours is clearly evident in the predictions made to 48 hours. The results of this investigation indicate that part of the generating mechanism for this oscillation resides in the method of treating the initial data.

An initialization difficulty was also discovered by Benwell and Bretherton (1968) in their investigation of the oscillation of the Bushby and Timpson (1967) model. Through a detailed linear analysis of the 10-level model, they identified the problem as an external gravity-inertia wave with a scale determined by the boundaries of the domain of integration. It was found to originate in the initial data in which terms in the linear balance equation had been neglected. These particular terms, although small, have a systematic effect in which their neglect generated the oscillation.

2. Diagnosis

Several examples of the temporal behavior of the average kinetic energy of the operational primitive equation model of the National Meteorological Center are presented in Fig. 1. For this model the kinetic energy is

$$K = \frac{1}{A} \int_{\sigma} \int_{A} \frac{1}{2g} (u^2 + v^2) \frac{\partial p}{\partial \sigma} \, dA \, d\sigma,$$

where g is the gravitational acceleration, p is pressure, σ is the vertical coordinate (a linear function of p), and A is the area of the forecast domain. Here u and v are the horizontal wind components in the x and y directions, respectively. A common feature in the forecast results is the increase in K during the first several hours. A maximum value is attained near the ninth hour of the forecast. The period of the dominant oscillation is approximately 10 hours.

Presented in Fig. 2 are the temporal variations of the average kinetic energy in the individual tropospheric layers (excluding the 50-mb deep boundary layer) of the model. All of those layers have equal mass and are numbered consecutively from bottom to top. Thus, layer 4 is the layer immediately below the material surface initially defined as the tropopause.

The results presented here have been normalized to a zero value at the initial time to better illustrate the relative variations in the absolute values. For this case, layers 2, 3, and 4 had initial kinetic energy values of 130, 290, and 760 kj m^{-2}, respectively. It is quite evident from Fig. 2 that the contribution to the oscillatory feature under consideration is almost exclusively from layer 4. The two stratospheric layers contributed in a similar way. The results indicated that the mechanism resided primarily in the region near the tropopause.

The data in the σ-system were interpolated (Shuman and Hovermale, 1968) back to the standard pressure levels, and the kinetic energy partitioned into its zonal and eddy parts (e.g., see Lorenz, 1955). The results for 200 mb for the February case for the initial and 12-hour forecast times are presented in Fig. 3 as a function of latitude. It is apparent that the increase in the total kinetic energy observed in the first 12 hours of the forecast is primarily attributable to an increase in its zonal component at the maximum wind levels. This was also evident in the other cases which were examined.

The results presented here indicate that the oscillation which is observed in the forecast model exists primarily in the zonal component of the kinetic energy in the vicinity of the tropopause. Since the presence of the phenomenon was independent of the initial state of the atmosphere, it was felt that the generating mechanism resided in the method of treatment of the data at the initial time rather than in the forecast model itself.

This hypothesis was further substantiated by certain verification statistics. The analyses and forecasts of wind and temperature are routinely verified by interpolating biquadratically from the grid points to observing station locations. The average results for the month of February 1970 are presented in Table 1. Notice that there exists a significant decrease of the wind speeds due to the initialization procedures.

Shuman and Hovermale (1968) have described the method of initialization which was employed at the National Meteorological Center. It can be briefly summarized as follows: The geopotentials are analyzed through an objective method of interpolating the information at the irregularly distributed station locations of the Northern Hemisphere to a regularly arranged grid. Then these fields are interpolated to the σ-surfaces. The balance equation was solved in each of the six σ-layers.

$$f\nabla^2\psi - 2\left(\psi^2_{xy} - \psi_{xx}\psi_{yy}\right) + \nabla f\cdot\nabla\psi = \nabla^2 Z, \tag{1}$$

where

$$\nabla Z = \nabla\phi + c_p\theta\nabla\pi \tag{2}$$

and

$$\pi = (p/p_o)^{R/c_p} .$$

Here f is the Coriolis parameter, ψ is the stream function, R is the gas constant for dry air, c_p is the specific heat of air at constant pressure, p is the pressure, p_o is 1000 mb, ϕ is the geopotential, ∇ is the horizontal Laplacian operator, and the subscripts refer to differentiation with respect to the independent variables. The potential temperature is denoted by θ, and from the hydrostatic relationship is

$$\theta = - c_p^{-1} \frac{\partial \phi}{\partial \pi} . \tag{3}$$

In order that Eq. (1) support valid solutions for the stream function, the equation must be elliptic, and thus

$$\nabla^2 z + \frac{1}{2} f^2 - \nabla f \cdot \nabla \psi > 0. \tag{4}$$

An iterative method was used to obtain a solution to the nonlinear Eq. (1). Condition (4) was satisfied periodically in the iterative procedure by suitably modifying the z field. The rotational wind component was obtained from this stream function and then the 12-hour forecast divergent wind component, verifying at the analysis time, was added to obtain the total wind. This wind field, together with the nonellipticized geopotential field, was used as the initial data for the forecast model.

It is evident from the above description of the method of data initialization that a significant source of imbalance between the mass and wind fields could exist. Specifically, this could occur in regions where the z-field was modified in order that condition (4) was satisfied. In those regions, the winds were in balance with a modified geopotential field, not with the original analyzed field which was used initially in the prediction. Ellsaesser (1968) has shown that in certain cases a substantial modification of the geopotential field is made in obtaining a solution to the balance equation. The resulting imbalance between such mass and wind fields would be reflected, although not exclusively, in the external gravity-inertia mode.

3. Numerical Experiments

In order to test the effects of the ellipticity criteria (4) on the forecast, it was decided that a more simplified prediction model would best serve this purpose. The primitive equation barotropic model which contains the external gravity-inertia wave solutions was used. Thus

$$u_t + \left(\frac{u^2 + v^2}{2} + \phi\right)_x - v\eta = 0 \tag{5}$$

$$v_t + \left(\frac{u^2 + v^2}{2} + \phi\right)_y + u\eta = 0 \tag{6}$$

$$\phi_t + (\phi u)_x + (\phi v)_y = 0 \tag{7}$$

where

$$\eta = v_x - u_y + F$$

Here u and v are the wind components in the x and y directions, respectively. The differencing method used was that described by Shuman and Stackpole (1969) for the operational model. The map projection and grid were identical to those of the operational model (Shuman and Hovermale, 1968). The average height (H) of the free surface was set to 10 km. The lateral boundary conditions were those also used by Shuman and Hovermale (1969) which assumed that the fluid was bounded by a free-slip wall.

Two predictions were made with this simple model using the 200-mb data for the February case. In prediction I the initial data was the wind field obtained from the balance equation, where $Z = \phi$, and the objectively analyzed geopotential field. Prediction II was similar to prediction I except the modified geopotential field resulting from the ellipticity criteria (4) was used instead. Thus, both predictions began with the identical wind field but with different geopotential fields. The analyzed 200-mb geopotential height is shown in Fig. 4 together with the difference of the two height fields. Notice that the elliptic criteria as imposed lowers the height field by as much as 120 meters south of the jet extending downstream from Japan. The difference between the geostrophic winds of the two height fields is as large as 50 m sec^{-1}.

The temporal behavior of the average kinetic energy for predictions I and II are shown in Fig. 5. For this model, the oscillation is more regular than in the baroclinic case with a period of 11.4 hours. Although the oscillation in prediction II has less amplitude than in prediction I, a significant amplitude still remains. This result was surprising since the initial data of prediction II was thought to be in the balance of Eq. (1). In both predictions, the total energy was closely conserved. Thus the oscillation represented a periodic exchange between kinetic and available potential energy.

The next step in this investigation was to test the initial data for balance with respect to the prediction model. That is, the model with its finite differences would be used to adjust the initial geopotential field by whatever amount is necessary to obtain a balance as defined by Eq. (1). The initial data of prediction II were used in this evaluation. It was assumed that the rotational wind field was correct. Then by satisfying the conditions $\nabla \cdot \mathbf{V} = (\nabla \cdot \mathbf{V})_t = 0$, as assumed in the derivation of Eq. (1), a required

modification to the geopotential field (ϕ') was obtained. The first condition, $\nabla \cdot \mathbb{V} = 0$, was satisfied since the winds were obtained directly from the given stream function. Eqs. (5) and (6) were modified by replacing ϕ by $\phi + \phi'$. The divergence equation was formed and $(\nabla \cdot \mathbb{V})_t$ set to zero. The resulting equation which was solved was

$$\nabla^2\phi' = [v\eta - \left(\frac{u^2+v^2}{2} + \phi\right)_x]_x - [u\eta + \left(\frac{u^2+v^2}{2} + \phi\right)_y]_y . \qquad (8)$$

At the lateral boundaries, ϕ' was set to zero.

In Fig. 6, the geopotential height field correction which was necessary to produce the intended balance is presented. It is primarily zonal in character with an average height of 65 meters in the vicinity of the pole. This field was then added to that used in prediction II and the forecast repeated--experiment III. The resulting kinetic energy temporal behavior is shown in Fig. 5. The oscillation had essentially vanished!

From an inspection of Fig. 6, it appeared that the stream function solution as obtained from the balance equation computer program had not fully converged. It can be shown that the first mode of the region of integration is one of the slowest to converge. Thus the balance equation solution was extended through additional iterative cycles and the resulting stream function was used to repeat experiment II. The results of this integration were the same as before--curve II in Fig. 5. Therefore, convergence had been obtained.

Upon inspecting the iterative procedure which was employed in solving the balance equation (1), it was found that the elliptic criteria (4) was imposed rather early in the iterative procedure. As can be seen from Eq. (4), this meant that an early estimate of the β-term, $\nabla f \cdot \nabla \psi$, was used. After criteria (4) was satisfied, this term in Eq. (1) was no longer updated in the iterative cycling. The initial estimate of the stream function which was used in the procedure was the field ϕ/f_o, where f_o is the Coriolis parameter at 45°N. Since the flow pattern was predominately zonal, this means that the magnitude of the β-term was underestimated in Eq. (1). Thus, the resulting zonal wind component was underestimated. To test this argument, the balance equation was solved again but this time with the ellipticity criteria applied later in the cycling procedure. The forecast results were identical to those obtained in experiment III. However, the speed of convergence in obtaining the initial stream function was less.

4. Discussion

The results of the barotropic experiments described in the preceeding section indicate that the generating mechanism of the oscillation observed in the temporal variation of the kinetic energy resided in the method of treatment of the initial data. The oscillation had its maximum amplitude when the analyzed geopotential height field and the balanced wind field were used. Using the ellipticized heights reduced the amplitude of the oscillation, but the major reduction was obtained when the β-term was more accurately accounted for in the iterative procedure. The existence of this term in the elliptic criteria (4) complicates the iterative method of obtaining the stream function. Underestimating the magnitude of the β-term in a predominantly zonal flow pattern resulted in an underestimate of the zonal winds. The effect of this in the prediction model was an imbalance between the mass and wind fields which produced a zonal wind acceleration (and an increase in the zonal kinetic energy). The initial imbalance in experiment II due to this error in the initial height field undoubtedly was reflected to a large extent in the first external mode formed by the boundary of the region of integration. The frequency, ω, of the gravity-inertia wave can be approximated by

$$\omega^2 = f^2 + c^2(k^2 + \ell^2)$$

where $k = 2\pi/L_x$ and $\ell = 2\pi/L_y$ are the wave numbers measured in the x and y directions and L_x and L_y are the corresponding wavelengths. For the case under consideration using $f = 10^{-4}$ sec^{-1}, $L_x = L_y = 2 \times 10^7$m (for the first mode) and $c^2 = gH = 10^5 m^2 sec^{-2}$, one obtains a period of 10.3 hours. This is near the value observed, 11.4 hours.

Because of the existence of the last term in Eq. 2, it was not feasible from an operational standpoint to obtain the ellipticized height fields for use initially in the six-layer baroclinic model. To do so would have significantly increased the computational time for initialization. However, the underestimate of the β-term in the procedure for the baroclinic model was measured. Using a method described in the barotropic experiments, the balance equation was solved applying the ellipticity criteria at later stages in the cycling procedure. The resulting forecast of the kinetic energy variations is shown in Fig. 1 (dotted curve) for 1200 GMT 10 February 1970. The oscillation has less amplitude. Furthermore, the kinetic energy growth rate during the first three hours is significantly less. It is suggested that the remaining kinetic energy growth which is evident in the first 10 hours of the forecast may be partially due to kinetic-to-potential energy conversions resulting from an initial state of mid-latitude systems by a baroclinic forecast model containing inaccurate simulations of friction and diabatic processes. Similar kinetic energy growth rates are characteristic of the operational forecasts made after August 23, 1971, which no longer utilize the balance equation in the initialization procedure.

Table 1

Analyzed wind differences and forecast wind errors for February 1970. ANAL refers to the analyzed values and 00-hr refers to the values after initialization. The first and second numbers given are the mean speed error and the root-mean-square vector error, respectively, in knots.

p(mb)	ANAL	00-hr	12-hr	24-hr	36-hr	48-hr
200	0.2/8.9	-7.7/20.9	-2.8/22.1	-7.5/30.9	-5.7/37.8	-5.0/40.2
250	-0.1/10.3	-6.4/20.8	-1.4/23.9	-5.5/32.2	-3.2/39.0	-2.4/43.6
300	-0.4/12.5	-4.7/21.7	-0.9/24.3	-3.6/30.5	-2.1/37.7	-0.3/42.9
500	-0.0/8.3	-1.3/14.1	-2.3/16.2	-2.1/20.5	-2.1/24.2	-0.8/27.3
700	-0.4/6.5	-0.8/11.4	-2.1/12.5	-1.9/15.2	-1.5/16.7	-0.1/18.8
850	-0.7/6.6	-1.1/13.8	-2.1/11.7	-2.9/13.9	-2.0/14.9	-1.6/17.3

REFERENCES

Benwell, G. R. R., and F. P. Bretherton, 1968: "A pressure oscillation in a 10-level atmospheric model." Quart. J. Roy. Meteor. Soc., 94, 123-131.

Bushby, F. H., and M. S. Timpson, 1967: "A 10-level atmospheric model and frontal rain." Quart. J. Roy. Meteor. Soc., 93, 1-17.

Ellsaesser, H. W., 1968: "Comparative test of wind laws for numerical weather prediction." Mon. Wea. Rev., 96, 277-285.

Lorenz, E. N., 1955: "Available potential energy and the maintenance of the general circulation." Tellus, 7, 157-167.

Shuman, F. G., and J. B. Hovermale, 1968: "An operational six-layer primitive equation model." J. Appl. Meteor., 7, 525-547.

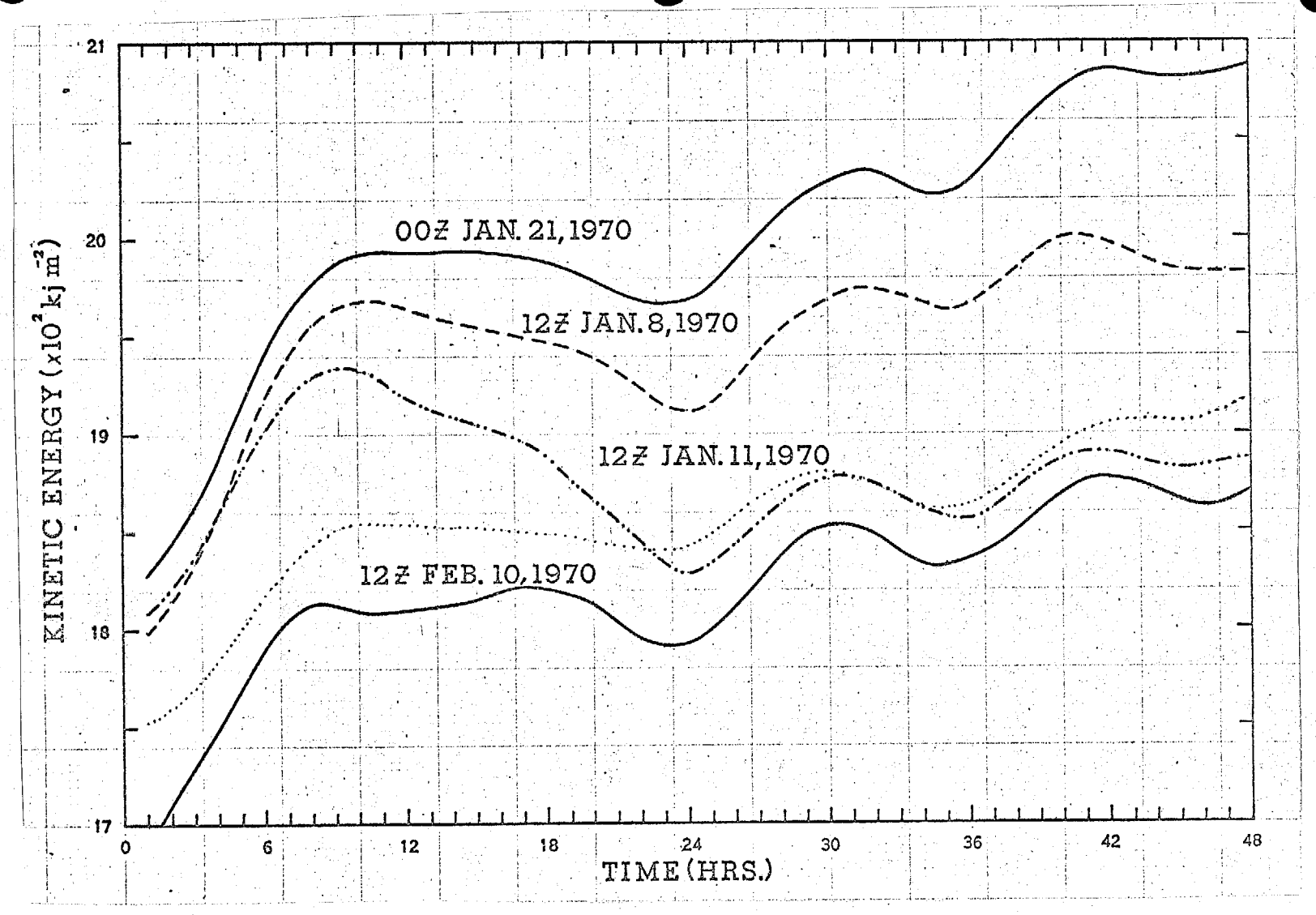

Fig. 1. Examples of the average kinetic energy as forecasted by the NMC six-layer primitive equation model. The dotted curve represents the modified forecast of 1200 GMT February 10, 1970.

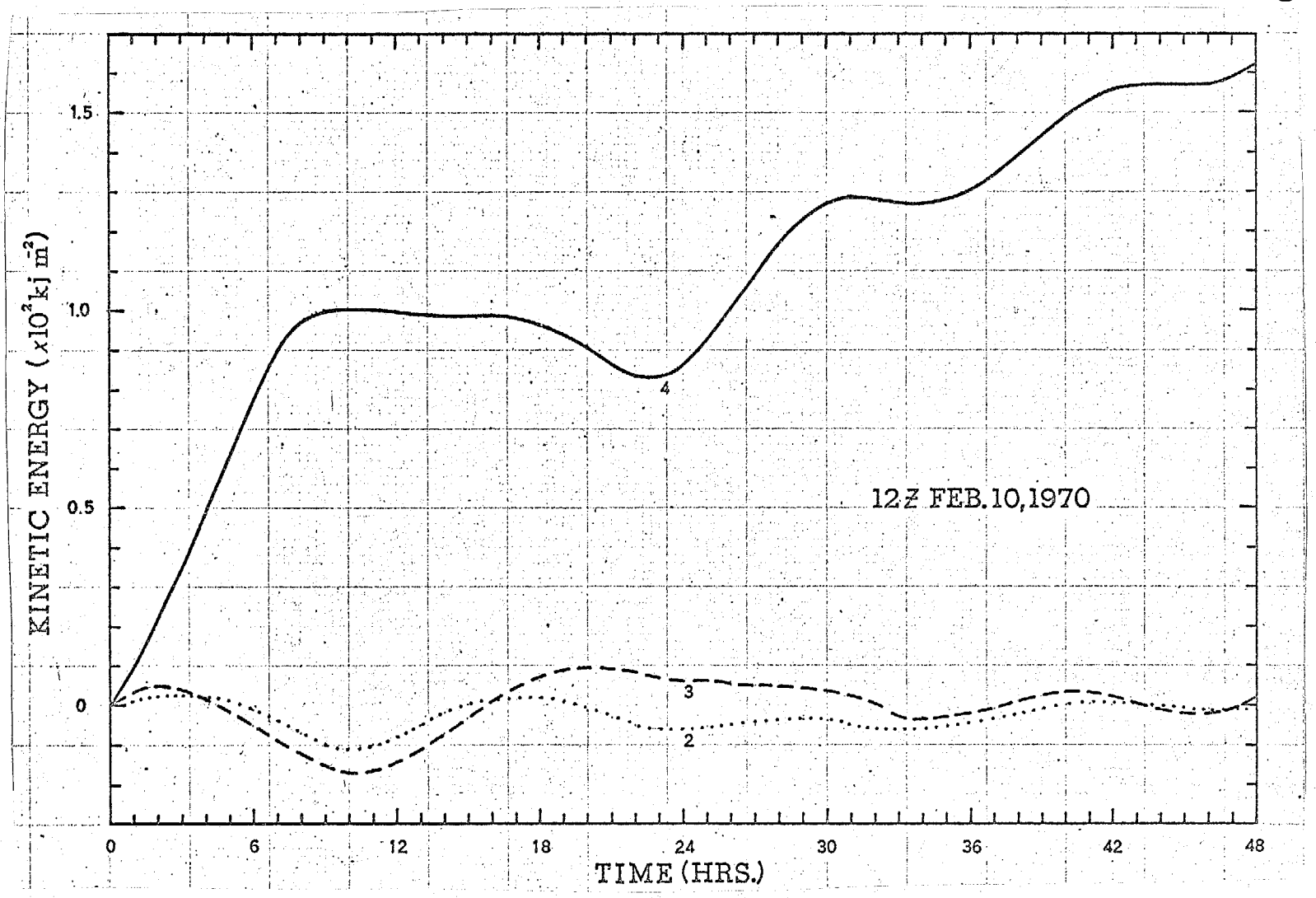

Fig. 2. The average kinetic energy variation as forecasted from 1200 GMT February 10, 1970 by the NMC six-layer primitive equation model for the three layers initially comprising the entire troposphere above the boundary layer. The values have been normalized as described in the text.

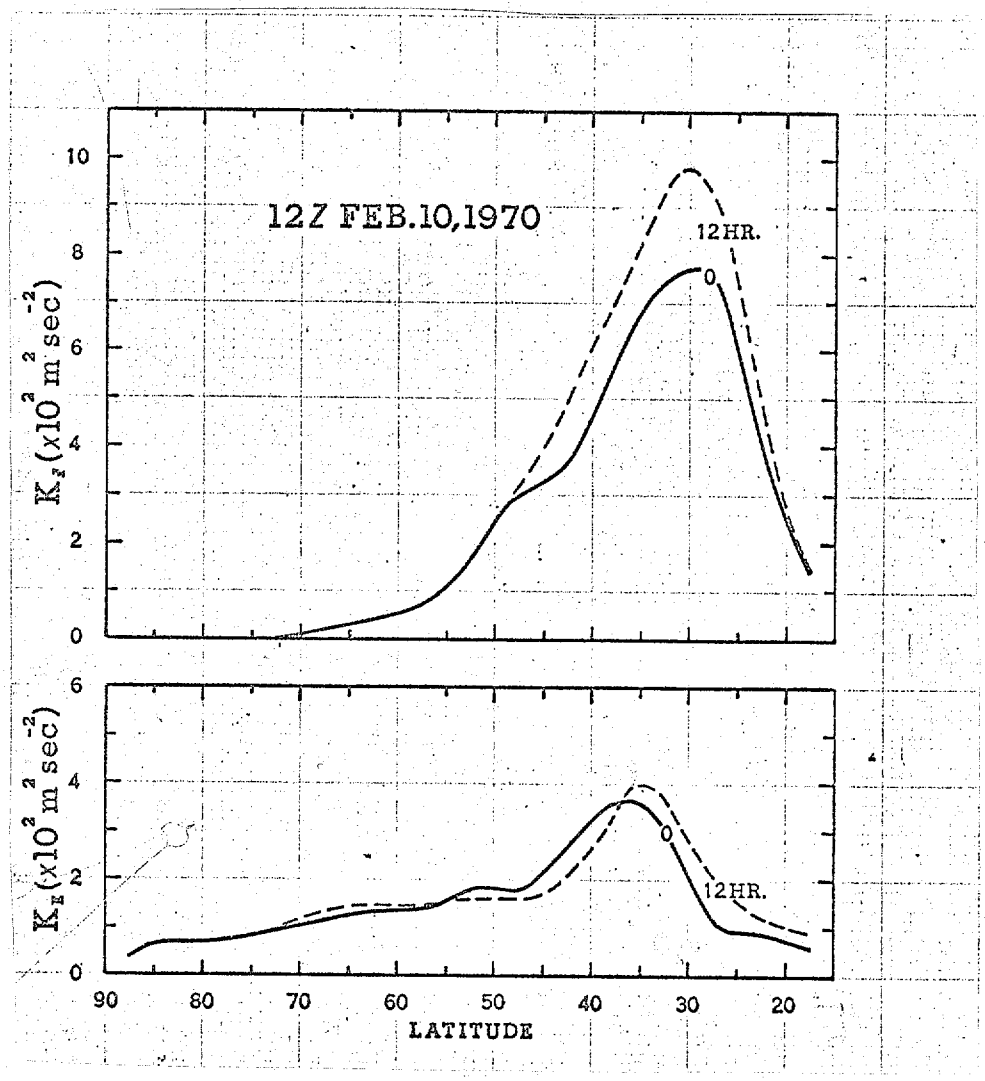

Figure 3. The average zonal kinetic energy (above) and eddy kinetic energy (below) as a function of latitude for the NMC six-layer primitive equation model for 0 hr (solid) and 12 hr (dashed). The initial data was for 1200 GMT February 10, 1970.

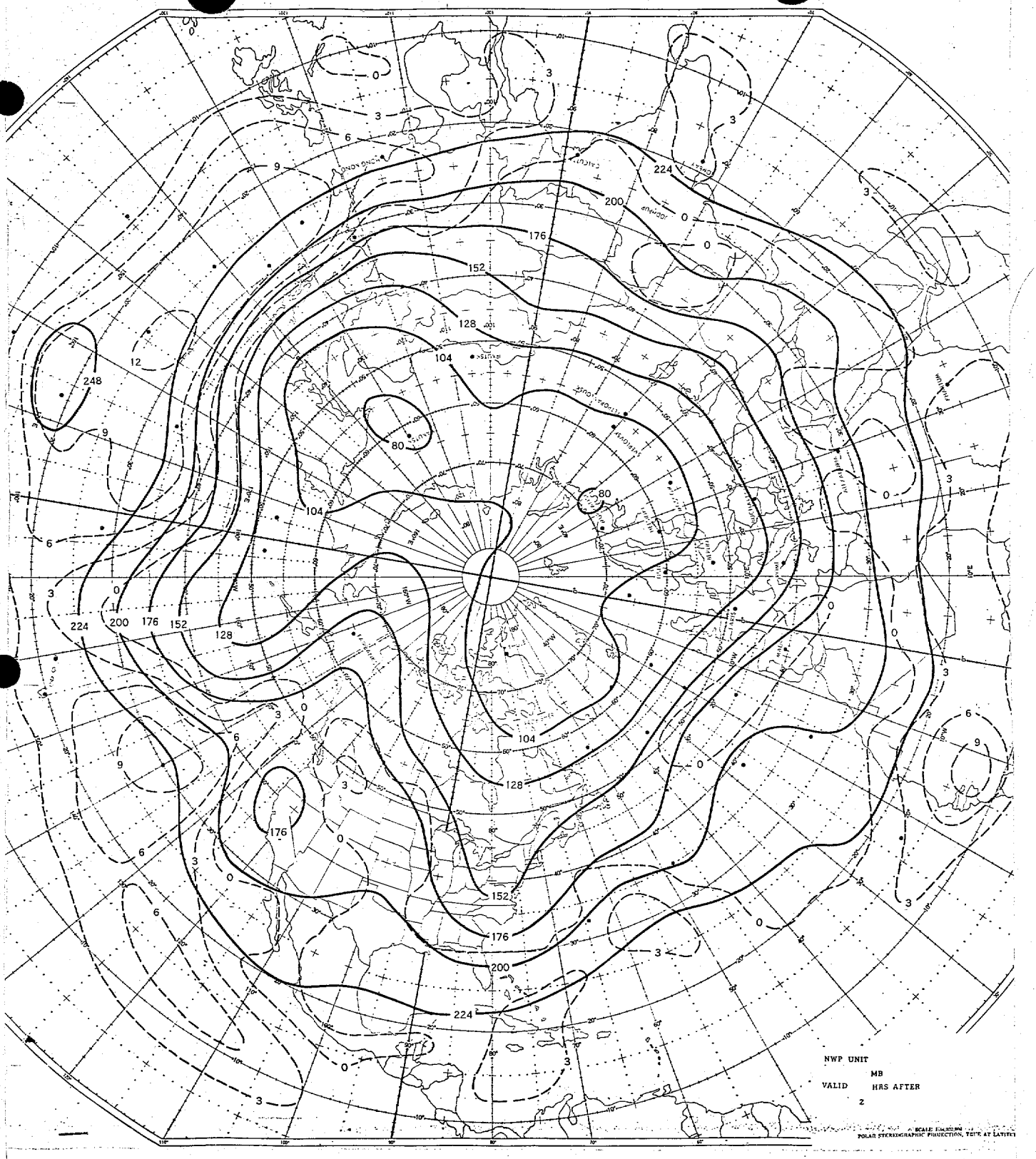

Fig. 4. The 200-mb analyzed geopotential height field (solid) and the analyzed minus ellipticized height field (dashed) for 1200 GMT February 1970. Units are decameters.

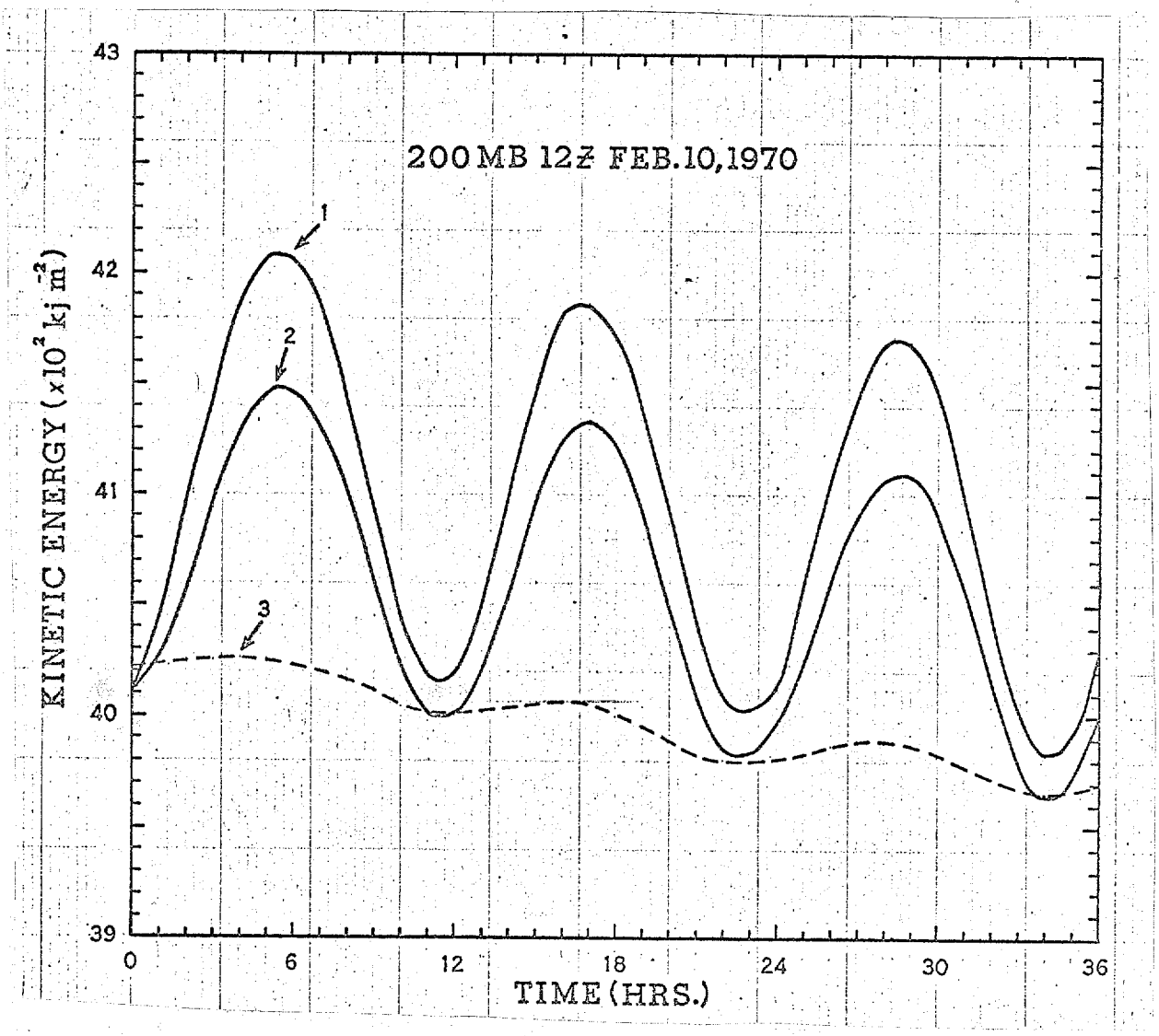

Fig. 5. The average kinetic energy as forecasted by the barotropic primitive equation model for experiments I, II and III.

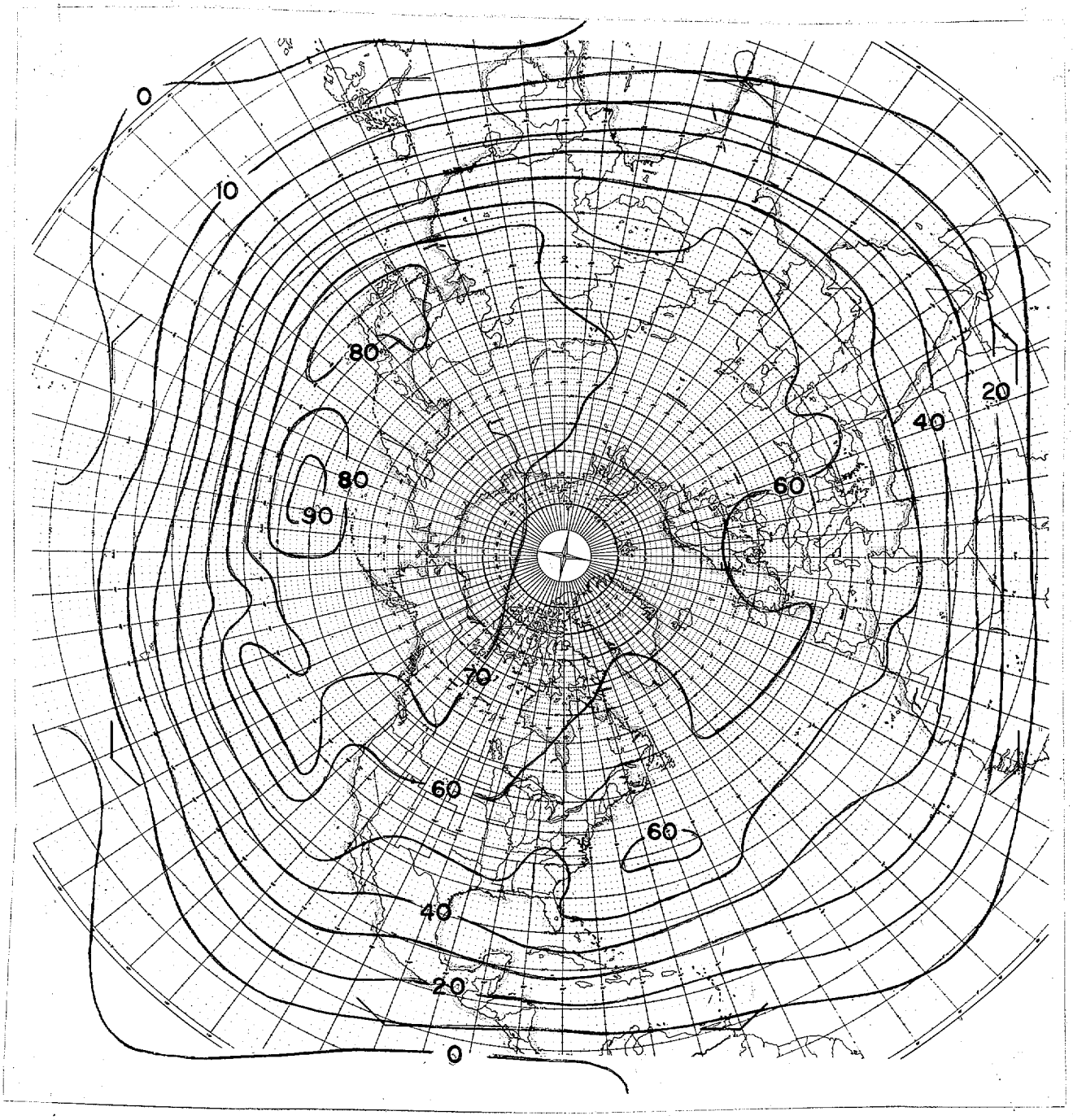

Fig. 6. The field of ϕ' in meters.